Directional Spectra of Surface Waves From Photographs

DENZIL STILWELL, JR., AND R. O. PILON

Naval Research Laboratory, Washington, D. C. 20375

A method is developed in which the spectrum of ocean surface waves may be deduced from oblique photographs. The method consists of determining the change of surface brightness with variations of surface slope and measuring the diffraction pattern of the photographic negative The diffraction pattern, obtained by a coherent optical processor, is then related to the two-dimensional wave number spectrum of the sea surface photographed. The conditions under which the optically derived spectrum is an accurate estimator of the ocean spectrum are discussed. The experimental method is applied to a nonstationary wave field exhibiting anomalously large spectral magnitudes. The two-dimensional spectrum of this wave field is displayed over a wavelength range of from 5 to 20 cm and an azimuth interval of about 90°.

Photographs of the ocean surface have been used in the study of waves since the development of photographic systems capable of imaging waves. Stereophotographs have been used to estimate the wave profile, the directional properties, and the spectrum of waves [*Neuman and Pierson*, 1966; *Pierson*, 1960]. The laborious process involved in the cross correlation of the pairs of photographs has hindered the use of stereophotos for the routine determination of spectra. Photographically recorded, sun glitter intensity distributions have been used to deduce many useful statistical features of surface slopes [*Cox and Munk*, 1954]. This method is highly successful in obtaining two-dimensional slope statistics but proves inappropriate for the deduction of more about profiles or spectral properties of the waves. *Barber* [1949] optically analyzed single photos of the ocean for the directional characteristics, but the necessary technology did not exist at the time to determine the spectrum. *Stilwell* [1969] reported the possibility that absolute spectral and directional information could simultaneously be determined from single photographs. Photographic negatives were optically analyzed by coherent optical techniques, and thus the need for computer analysis of time series and point by point scanning techniques was eliminated.

A photographic negative proves to be quite appropriate in the study of ocean surface waves in that a miniature version of what the eye perceives can be reconstructed in the laboratory and subjected to a detailed examination. The photo can be taken from any convenient platform, be it a ship, helicopter, tower, aircraft, or spacecraft. Each frame of the resulting film constitutes a tremendous store of information pertaining to an area of the ocean at a particular instant of time. Since the camera can take pictures rapidly and the platform can be quite mobile, an immense amount of data can be generated about the temporal and spatial variations of the wave field. As a result of the huge amounts of information recorded, the minimal interference with the observed field, and rapid sampling in space and time the statistical precision with which a spectrum may be obtained from photographs is extended over that attainable by most alternative techniques.

The development of coherent optical processing techniques has made the analysis of photographic negatives a practical method of deducing wave information. The technique illuminates the film with the collimated monochromatic light from a laser and measures the resulting diffraction pattern. The diffracted light is passed through a lens that in the absence of the film focuses all the light to a spot in the back focal plane. With the film perturbing the light amplitude field a distribution of light intensity is generated that can be related to the wave spectrum of the original scene. The reason that the resulting intensity distribution can be related to the spectrum is that the transfer function from the front to the back focal plane of any lens is functionally identical to a Fourier transform. Since the square of the Fourier transform is directly proportional to the spectrum, the optical transform accomplishes in an analog manner the complex mathematical procedure.

A spectral representation can greatly simplify the study of important features of a process. A spectrum, although it constitutes significantly less information than the original data, retains many of the salient features in a form more amenable to interpretation. An ocean surface for which a spectrum can be defined must consist of an unbroken surface with a smooth profile. Precisely, the spectrum is undefined at wind speeds beyond the onset of whitecapping because the surface becomes multivalued. Practically, the utility of the spectrum diminishes owing to the effects of the broken water only at a scale of wavelengths smaller than the scale of the disturbed areas. The spectral estimates for the longer water waves are not necessarily degraded.

This investigation is undertaken to develop an operational photographic system capable of remotely sensing the ocean surface and providing a quantitative estimate of the surface wave spectrum. To accomplish this, it is necessary to establish the geometrical relationship between the surface point and its image on the film, obtain a relationship between some surface descriptor and the film exposure, relate the optical diffraction pattern to the modulation effects introduced by the film, and finally, derive the equations connecting the measurement of the diffraction pattern to the spectrum of the waves. In the course of this procedure it is necessary to explicitly state the spectrum in a form appropriate to the two-dimensional nature of the data, analyze the characteristics of wave visibility as dependent on the illumination conditions and the surface variables, and incorporate the effects of the imaging system.

WAVE VISIBILITY IN TWO DIMENSIONS

The subject of the visibility of waves is obviously of primary importance to this technique. Most of the physically important features of wave visibility arise in the simplest case.

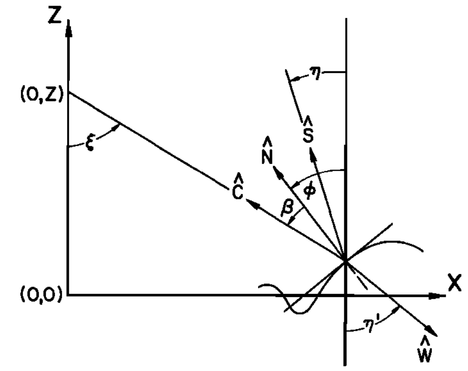

Fig. 1. The two-dimensional geometry showing the directions of the sky and water rays that reach the camera.

Figure 1 sketches the geometry relating the surface point and the camera for a line profile of the surface. The light emanating from any point on the ocean surface directed toward the camera must consist of only two portions, that reflected by the surface from the sky from the direction $\hat{S}$ and that refracted by the surface from the direction $\hat{W}$. In addition to these two light contributions there is another, that light scattered from the intervening medium toward the camera. With the most convenient choice of units

$$U(\xi, \phi) = \Gamma(\beta)L(\eta) + \Lambda(\eta') + s(\xi) \tag{1}$$

where Γ is the Fresnel reflection coefficient, L is the sky luminance, s is the scattered light, and Λ is the upwelling luminance above the water surface that originated underneath the water. The use of the terminology of luminance instead of that of radiance is somewhat arbitrary and is selected simply because the films and instruments used in this work have a light spectral response more closely matching that of the eye than the uniform response useful in radiant measures.

The quantities introduced in (1) are all polarization dependent. For explicitness, each of these quantities should be subscripted with an appropriate letter denoting either horizontal or vertical polarization. The Fresnel reflectivity curves show that only for horizontal polarization is the reflectivity a unique function of the incidence angle. It will be assumed that a polarizer is included in the camera system, which will exclude vertically polarized light, and no subscripts will be used.

The scattering term s can only obscure the wave information. This phenomenon is the primary limitation to obtaining good photographs of the ocean. It incorporates such observables as fog, clouds, haze, and smog. Of necessity, this term will be disregarded in the theoretical arguments, although it cannot be ignored in the experimental design. Often it is necessary to photograph the surface from a much lower altitude than would otherwise be desirable because of a cloud deck or a hazy atmosphere. As a result, wide-angle lenses must be used in situations where long focal lengths and high altitudes would be preferred.

Writing (1) in terms of the angles ξ and ϕ gives

$$\begin{aligned} U(\xi, \phi) &= \Gamma(\xi - \phi)L(\xi - 2\phi) \\ &\quad + \Lambda\{\phi + \sin^{-1}[(1/n)\sin(\xi - \phi)]\} + s(\xi) \end{aligned} \tag{2}$$

from which the functional derivatives

$$U_\xi = \Gamma'L + \Gamma L' + \Lambda' f' \tag{3}$$

and

$$U_\phi = -\Gamma'L - 2\Gamma L' + \Lambda'(1 - f') \tag{4}$$

result, subscripts denoting partial differentiation and primes denoting differentiation with respect to the argument. The quantity f is used to denote the arc sine function occurring in the upwelling light term, and n is the index of refraction of the water. A close examination of these equations reveals most of the observable features of the visibility of waves and the consequent imagery. Highly discontinuous luminance functions yield maximal wave contrast. Such light distributions, however, either overemphasize the existence of particular slopes or destroy any unique relationship between a given slope and its brightness. Only monotonic or at worst slowly varying distributions can yield a faithful representation of the surface onto the film. Near vertical incidence, both the water reflectivity and its derivative assume nearly zero magnitudes. In this case, wave visibility is almost completely dominated by upwelling light. Because the sun usually is not directly overhead, it is possible to image waves with the camera looking straight down, but unfortunately the wave visibility is generally quite small. Only in the instance of large wave slopes with the sun low in the sky or obscured is this mode of operation useful. Usually, to obtain sufficient wave visibility with an absence of reflected sun, an aspect angle considerably removed from the nadir is required. Equation 4 shows that at some aspect angle there may be no wave visibility. In many cases this angle is of the order of 25°–30° from the nadir. As a result, rather extreme obliquity is often necessitated to image waves of small angular amplitude. Although oblique incidence introduces perspective distortion, it is still possible to obtain good estimates of the spectrum.

WAVE VISIBILITY IN THREE DIMENSIONS

To obtain the wave number spectrum requires that the geometry of the ocean wave imaging and visibility be expressed in terms of the wave amplitude and direction. The experimental configuration for the scene photography is shown from a side and top view in the two parts of Figure 2. The camera is positioned at a height Z above the mean level of the water surface with the boresight angle incident obliquely at the angle ξ. The camera has the field of view $\Delta\xi$ in the elevation plane and the angle $\Delta\alpha$ in the azimuth plane. The trapezoidal area outlined is imaged onto the rectangular for-

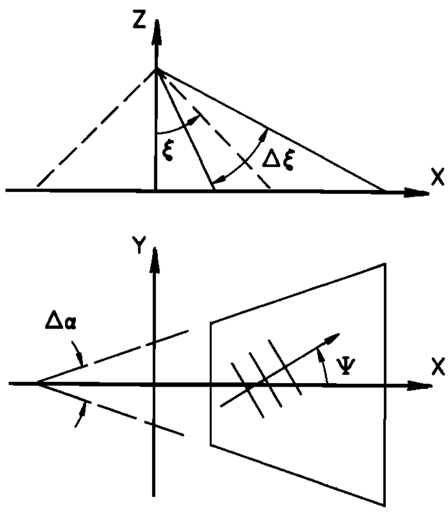

Fig. 2. Two views of the region imaged by the camera system.

mat of the film. The lines oriented at an angle Ψ represent a wave packet. Reflection and refraction take place in a plane that includes the surface normal angle and the camera look direction. If the normal angle to the surface is allowed to assume deflections out of the plane of Figure 1, three new angles are required to describe the local geometry. The angles between the horizontal projections of $\hat{S}$, $\hat{N}$, and $\hat{W}$ with the X axis are denoted as ζ, Ψ and ζ', respectively. Appendix 2 shows a sketch of this geometry and collects the formulas for the determination of the angles.

In this three-dimensional case the functional dependence of the light intensity impinging the camera is

$$U(\xi, \phi, \Psi) = \Gamma(\beta)L(\eta, \zeta) + \Lambda(\eta', \zeta') \tag{5}$$

where the expression is written without the α dependence and scattered light is ignored. The wave visibility is then

$$U_\phi = \Gamma_\beta L \beta_\phi + \Gamma(L_\eta \eta_\phi + L_\zeta \zeta_\phi) + \Lambda_{\eta'} \eta'_\phi + \Lambda_{\zeta'} \zeta'_\phi \tag{6}$$

where subscripts denote partial differentiation. The β, η, ζ, η', and ζ' derivatives can be evaluated from the formulas in Appendix 2. To simplify the equations that result, it is convenient to assume that ϕ is small. As a result of this assumption, each of the derivatives involves a cos Ψ factor that represents the totality of the Ψ dependence for an azimuth interval of about $\pm 45°$. Thus the wave visibility can be factored into a product of an azimuthal term and a term involving the normal angle and the camera angle. Furthermore, the ζ_ϕ' and ζ_ϕ terms are considerably smaller than the other derivatives. In conjunction with the physical assumption that L_ζ and Λ_ζ are generally small in relation to L_η and Λ_η' an additional simplification of (6) occurs, viz.,

$$U_\phi = \cos\Psi\,[-\Gamma' L - 2\Gamma L' + \Lambda'(1 - f')] \tag{7}$$

where the primes again represent argument differentiation and f is the arc sine function for (2). The net result of these equations is that the camera system is sensitive primarily to the x component of the slope of the wave. Thus the brightness of a point on the ocean can be written as

$$U(\xi, \alpha) = U_0(\xi) + U_\phi(\xi)\phi(\xi, \alpha) + O(\phi^2) \tag{8}$$

In order to evaluate the wave visibility as expressed in (7) it is necessary to obtain a wide-angle photograph that includes both the sky and the ocean over the angles of interest. Although this can be done by photographing sections of the sky and ocean and normalizing with the light intensities in the overlapping regions, it is most conveniently accomplished with a fisheye lens. With this lens a full hemisphere can be photographed with little effect from vignetting, and the relative intensities between any two points can be accurately measured. Then since the reflectivity is given by the formula

$$\Gamma(\beta) = \frac{\sin^2(\beta - \beta')}{\sin^2(\beta + \beta')} \qquad \sin\beta = 1.34\sin\beta' \tag{9}$$

all the terms can either be calculated or measured. The upwelling term is calculated from an integrated version of (5) in which the ϕ variation is averaged out by smoothing over a substantial $\Delta\xi$ interval.

OPTICAL TRANSFORMS

The optical analysis of the negative on the optical bench uses the relationship between the light amplitudes in the two focal planes of any lens. A lens has a transfer function between its front and back focal planes that becomes a pure Fourier transform when it is used with collimated monochromatic light. When a positive transparency of a scene is inserted into the collimated beam, an image is reconstructed immediately following the film that is to within the camera-film resolution and fidelity limitations a replica of the light distribution that existed at the camera from the scene. The net effect of the recording is to reconstruct this aerial image. In water wave photography the small amplitudes of the waves, an inherent characteristic of water waves in the gravity range, allows a linear relation between the reconstructed light amplitude and the wave normal angle. Thus the light amplitude distribution in the other focal plane becomes the Fourier transform of the surface normal angle variations. The light intensity is proportional to the energy spectrum of the waves.

Figure 3 is a sketch of the optical system used to obtain transforms. For simplicity and signal to noise considerations this system does not use a collimated laser beam; thus some phase distortions are introduced into the transform, but the light energy distribution in the Fourier plane is not affected. The lens images the spatial filter pinhole into the Fourier plane and results in a nearly Gaussian intensity distribution, since the axial intensity of light from a laser is often close to Gaussian. Likewise, the intensity of light at the scene plane is closely approximated by a two-dimensional Gaussian distribution. Thus the weight function introduced in (A4) of Appendix 1 is introduced by the optical system.

PHOTOGRAPH SPECTRUM

With the wave visibility as a function of the angular excursion and direction of the wave it is now possible to proceed in the determination of the spectrum. First, it is necessary to obtain explicit formulas relating the film parameters to the observed light distributions. The light intensity at the transform plane is given explicitly [*Goodman*, 1968] by

$$I_f(x_f, y_f) = (\lambda F)^{-2} \left| \iint_{-\infty}^{\infty} A(x, y)t(x, y) \cdot \exp\,[-(2\pi i/\lambda F)(xx_f + yy_f)]\,dx\,dy \right|^2 \tag{10}$$

where x and y are the coordinates centered at the scene and the x_f and y_f are the coordinates in the transform plane centered at the image of the spatial pinhole filter. Here λ is the optical wavelength (632.8 nm), $t(x, y)$ is the amplitude transmission coefficient of the film, and $A(x, y) = A_0 G(x, y)$ is the amplitude of light impinging the film from the laser. The light amplitude transmission is related to the optical density D of the film by

$$t(x, y) = 10^{-1/2[D(x,y)]} \tag{11}$$

The phase factor, which should be included in the $t(x, y)$ term, is to be eliminated by the use of a liquid gate and will not be considered. (As a first approximation such phase effects introduce only a white noise spectrum and may be ignored with

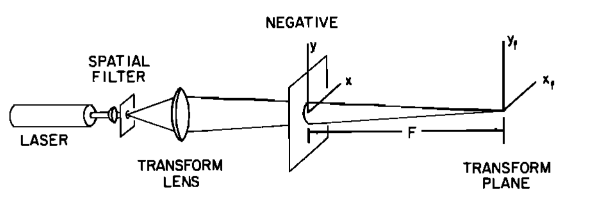

Fig. 3. The optical analysis system.

strong signals.) With the image recorded at an exposure level within the linear range of the characteristic curve for the emulsion of the film the optical density resulting from the exposure $U(x, y)$ is

$$D(x, y) = \gamma \log_{10} [qU(x, y)] = \log_{10} [qU(x, y)]^{\gamma} \quad (12)$$

where γ is the slope of the characteristic curve and q is a light sensitivity constant of the film to the incident light. The q factor is not, nor need not be, known explicitly, since subsequent theoretical development will use relative exposures only, causing cancellation of the unknown q. The exposure of (8) can be written as

$$U(x, y) = U_0(x) + U_\phi(x)\phi(x, y) \equiv U_0(x)[1 + \mu\phi(x, y)] \quad (13)$$

The function $U_0(x)$ can be measured by scanning the scene film with a densitometer having an aperture that averages out the effects due to waves. Equation 7, expressed in terms of the film coordinates, gives the wave sensitivity.

Substituting these expressions into (10) and using the operator $\mathfrak{F}\{\ \}$ to denote a two-dimensional Fourier transform gives

$$I_f(x_f, y_f) = (\lambda F)^{-2} A_0^2 \,|\mathfrak{F}\{Gt_0\} - (\gamma/2)\mathfrak{F}\{G\mu t_0\phi\}|^2 \quad (14)$$

where G is the Gaussian function of (A4) and where

$$t_0 = [qU_0(x)]^{-(\gamma/2)} \quad (15)$$

and

$$\mu(x) = U_\phi(x) \cos \Psi / U_0(x) \quad (16)$$

where A_0 is the peak amplitude of the laser light just before the negative. When $I_f(x_f, y_f)$ is expanded,

$$I_f(x_f, y_f) = (\lambda F)^{-2} A_0^2 [\mathfrak{F}^2\{Gt_0\} - \gamma \,\mathrm{Re}\, (\mathfrak{F}\{Gt_0\mu\phi\}\,\mathfrak{F}\{Gt_0\}) + \tfrac{1}{4}\gamma^2 \,|\mathfrak{F}\{Gt_0\mu\phi\}|^2] \quad (17)$$

The three terms in parentheses lend themselves to the following interpretation. The first two terms vanish exponentially with distance from the origin because of the weighting introduced by the Gaussian function. The first term has no appreciable wave number components at values large in relation to σ^{-1}, and although the second term may have, it is strongly attenuated by the Gaussian. The net result is that the first two terms give a narrow Gaussian light distribution at the center of coordinates in the transform plane (a dc term). The third term in (17) incorporates all the spectral information of the waves that can be retrieved. This term can be altered by the procedure used for (A7) to give

$$\mathfrak{F}\{G\mu t_0\phi\} = \mathfrak{F}\{G\mu t_0\} * \bar{\phi} \equiv |G\mu t_0| \langle\bar{\phi}\rangle \quad (18)$$

where the overbar indicates a Fourier transform. The convolution denoted by the asterisk smooths the Fourier transform by averaging in spectral space with a window given by the transform of the $G\mu t_0$ product. Since it is necessary to smooth the spectrum in order to obtain results that are not wildly varying, the above smoothing detracts little if any from the utility of the results.

It is now possible to express the light intensity outside the dc term in terms of measurable quantities and the spectrum. When I' is the light intensity outside the dc term,

$$I'(x_f, y_f) = (\lambda F)^{-2} A_0^2 \tfrac{1}{4}\gamma^2 |G\mu t_0|^2 \langle\bar{\phi}^2\rangle \quad (19)$$

The spectrum is defined to be

$$\Phi(\mathbf{k}) = \int_{\mathbf{k}}^{\mathbf{k}+\delta\mathbf{k}} \langle\bar{\phi}^2(\mathbf{k})\rangle \, d\mathbf{k} \quad (20)$$

The elemental region $\delta\mathbf{k}$ is that corresponding to the effective aperture utilized in the scene plane, explicitly

$$\delta k_x\, \delta k_y\, \delta x\, \delta y = 1 = [\delta x_f\, \delta y_f/(\lambda F)^2]\, \delta x\, \delta y \quad (21)$$

where

$$\delta x = [(G\mu t_0)_{\max}]^{-1} \int_{-\infty}^{\infty} G\mu t_0 \, dx \quad (22)$$

$$\delta y = [(Gt_0)_{\max}]^{-1} \int_{-\infty}^{\infty} Gt_0 \, dy \quad (23)$$

The measurement of the light intensity of (19) involves the use of a physical aperture of area Δa. Since this measurement is made in the Fourier analysis plane, the aperture corresponds to a two-dimensional wave number interval $\Delta\mathbf{k}$ different from the $\delta\mathbf{k}$ used in the definition of the spectrum. Therefore

$$\int_{\Delta\mathbf{k}} I'(x_f, y_f)\, dk_x\, dk_y = (\lambda F)^{-2}(\tfrac{1}{2} A_0\gamma\, |G\mu t_0|)^2 \int_{\Delta\mathbf{k}} \langle\bar{\phi}^2\rangle \, dk_x\, dk_y \quad (24)$$

$$(\lambda F)^{-2} \int_{\Delta a} I'(x_f, y_f)\, dx_f\, dy_f = (\lambda F)^{-2}(\tfrac{1}{2} A_0\gamma\, |G\mu t_0|)^2 \frac{\Delta\mathbf{k}}{\delta\mathbf{k}} \langle\Phi(\mathbf{k})\rangle$$

with

$$\langle\Phi(\mathbf{k})\rangle = (1/\Delta\mathbf{k}) \int_{\mathbf{k}}^{\mathbf{k}+\Delta\mathbf{k}} \Phi(\mathbf{k})\, d\mathbf{k} \quad (25)$$

which represents a smoothed spectral estimate. The ratio

$$\frac{\Delta\mathbf{k}}{\delta\mathbf{k}} = (\lambda F)^{-2}\, \Delta x_f\, \Delta y_f\, \delta x\, \delta y = (\lambda F)^{-2}\, \Delta a\, \delta x\, \delta y \quad (26)$$

represents the equivalent number of chi-square variables contributing to the smoothed estimate of the spectrum.

Identifying

$$\mathcal{R}(x_f, y_f) = \int_{\Delta a} I'(x_f, y_f)\, dx_f\, dy_f \quad (27)$$

with the measurement of the light power at the wave number plane and

$$\mathcal{R}_0 = \Delta a_0 |A_0 G t_0|^2 \quad (28)$$

with the light power just after the scene plane gives

$$\langle\Phi(\mathbf{k})\rangle = \frac{\Delta a_0}{\Delta a} \left(\frac{2}{\gamma}\right)^2 \mu^{-2} \frac{(\lambda F)^2}{\delta x\, \delta y} \frac{\mathcal{R}(\lambda F k_x, \lambda F k_y)}{\mathcal{R}_0} \quad (29)$$

The effective magnitude of the modified wave visibility is

$$\mu = \left(\int_{-\infty}^{\infty} Gt_0\, dx\right)^{-1} \int_{-\infty}^{\infty} G\mu t_0\, dx = \frac{U_\phi(x_0)}{U_0(x_0)} \cos\Psi \quad (30)$$

where x_0 is the effective center of the transformed area.

OCEAN SPECTRUM

The spectrum of (29) could represent an infinitude of actual ocean surfaces. The expression involves only angular measurements (even the $\delta x\ \delta y$, although they are physical distance on the negative, really refer to the effective angular interval over which the ocean scene was recorded). The demagnifications M_x and M_y of lengths ΔX and ΔY onto the film as Δx and Δy provide the required scaling factors to uniquely determine the spectrum of the ocean surface waves (see Appendix 3).

$$\begin{aligned} M_x \Delta x &= \Delta X \qquad & M_x &= (Z/F_1) \sec^2 \xi \\ M_y \Delta y &= \Delta Y \qquad & M_y &= (Z/F_1) \sec \xi \end{aligned} \tag{31}$$

where Z is the height of the camera above the mean water level and F_1 is the focal length of the camera.

The fact that neither M_x nor M_y is constant creates the problem of perspective variation. If a single sinusoid were envisioned on the ocean, the film would show a spatial frequency variation across the film, the change in spatial frequency being related to the angular interval $\Delta\xi$ (or $\Delta\alpha$) analyzed. Only three things can be done to reduce the smearing introduced by perspective change. The camera must look toward the nadir, the angular intervals $\Delta\xi$ and $\Delta\alpha$ must be small, or the film must be curved when it is placed on the optical bench in a way to cancel the effects of perspective. All three of these techniques are useful, but for the purposes of this paper the smearing is to be ignored, and only the perspective effect on the demagnification is to be accounted for. The effective demagnification factors are given by

$$\begin{aligned} \langle M_x \rangle &= \left(\int_{-\infty}^{\infty} Gu'{t_0}\, dx \right)^{-1} \int_{-\infty}^{\infty} M_x(x) Gu'{t_0}\, dx \\ &= (Z/F_1) \sec^2 \xi_0 \\ \langle M_y \rangle &= \left(\int_{-\infty}^{\infty} Gu'{t_0}\, dx \right)^{-1} \int_{-\infty}^{\infty} M_y(x) Gu'{t_0}\, dx \\ &= (Z/F_1) \sec \xi_0 \end{aligned} \tag{32}$$

and the effect of perspective in α is ignored.

With the above scaling factors the equations of Appendix 3 are appropriate with M_z taken equal to unity. The complete equation for the ocean spectrum in terms of measurable parameters is

$$\Phi_{\text{ocean}}(K, \Psi) = \left[\frac{Z^2}{F_1^2} \sec^3 \xi_0 \frac{\Delta a_0}{\Delta a} \frac{4}{\gamma^2} \left(\frac{U_0}{U_\phi} \right)^2 \frac{(\lambda F)^2}{\delta x\ \delta y} \right] \cdot \frac{\mathcal{R}(\kappa K, \Psi)}{\mathcal{R}_0} \sec^2 \Psi \tag{33}$$

with

$$\kappa = (F/F_1) \lambda Z \sec \xi_0 (\sec^2 \xi_0 + \tan^2 \Psi)^{1/2} \tag{34}$$

where Z is the height of the camera above the ocean, F_1 is the camera focal length, and ξ_0 is the effective depression angle of the camera for the region of the photograph analyzed. Here Δa_0 is the photomultiplier (PM) aperture used in measuring the light power $\mathcal{R}_0$ at the scene plane on the optical bench; Δa is the corresponding aperture for $\mathcal{R}$, U_0/U_ϕ is the normalized wave visibility from (8), λ is the laser wavelength, F is the effective focal length of the optical bench lens, and $\delta x\ \delta y$ is the effective area of the photograph analyzed. Thus the optical techniques prescribed here result in an absolute estimator of the ocean spectrum.

SUBRESOLUTION WAVES

Waves on the ocean surface of a scale smaller than the resolution allowed by the camera-film-air turbidity effects can introduce a modification of the effective luminance functions from that which would be determined from a glassy smooth sea. The subresolution waves, especially those in the capillary regime, can have significant slopes. Since they are unresolved on the film, the intensity variations of the sky are partially smoothed. This effect can be observed by examining the reflection of a cloud in a ruffled water surface. As a result the small waves can smooth the sky luminance distribution and allow the use of photographic procedures on days in which the sky is far from a monotonic luminance function. Contingent only on the distribution of subresolution waves being homogeneous, the effective luminance distributions may extend the environmental conditions under which optical transforms are useful.

LONG-WAVELENGTH SPECTRUM

Optical analysis performs exactly and very rapidly a mathematical transformation that is otherwise lengthy and somewhat difficult. The limitations of sea photo analysis basically reside in the difficulty encountered in obtaining an appropriate photograph. The variation of the magnification across the photo is the major difficulty in analyzing long water waves when it is not possible to photograph the surface from an altitude sufficiently high to reduce perspective distortion to permissible values. It is possible to exact the low-frequency content from a photo by resorting to scanning techniques such as a microdensitometer coupled into a computer in which the coordinates can be corrected point by point. Such techniques are of much value in retrieving long-wavelength information from low-altitude photos.

It is also possible to obtain the long-wavelength spectrum from low altitudes with a strip camera, in this case an aircraft outfitted with a camera in which the film moves in synchronization with the ground speed. This system can image long strips of film from very low altitudes with no perspective distortion along track. Only a small angular region $\Delta\xi$ is imaged onto the film, and the aircraft motion scans in X. If the wave visibility is established as outlined in this paper, the optical spectrum can be developed from the strip film for wave numbers in the direction of the strip. This circumvents the normal sea photo analysis difficulty of variation of magnification.

EXPERIMENTAL RESULTS

Figure 4 represents a series of spectra observed at the Naval Undersea Center tower off Mission Beach in San Diego on October 5, 1971. The camera, a 35-mm Nikon with a 50-mm lens, was positioned 19 m above the mean water level. The figures show the rapidly changing spectrum of a highly nonstationary wave field. At about 1802 UT the previously dead calm suddenly changed into a mild wind of about 4–6 m/s. The anemometer records indicate that the direction and the magnitude of the wind did not vary greatly during the interval analyzed. In addition, since the optically analyzed region of the film corresponded to an elliptical area on the ocean with major and minor axes of 9 and 7 m, the wave field may well have been inhomogeneous. The development of the spectrum with time subsequent to the step function of wind velocity is plotted. The spectral amplitude scale is in db above a level of $0.25 \times 10^{-2}\ \text{cm}^2\ \text{rad}^2$. The signal to noise ratio varies, since part of the low-frequency trend would have to be considered noise.

The spectrum exhibits an apparent overshoot of the equilibrium level attained in the last times illustrated. The peak propagates to longer wavelengths, and only the 18h 06m 15s spectrum shows a significant region not showing

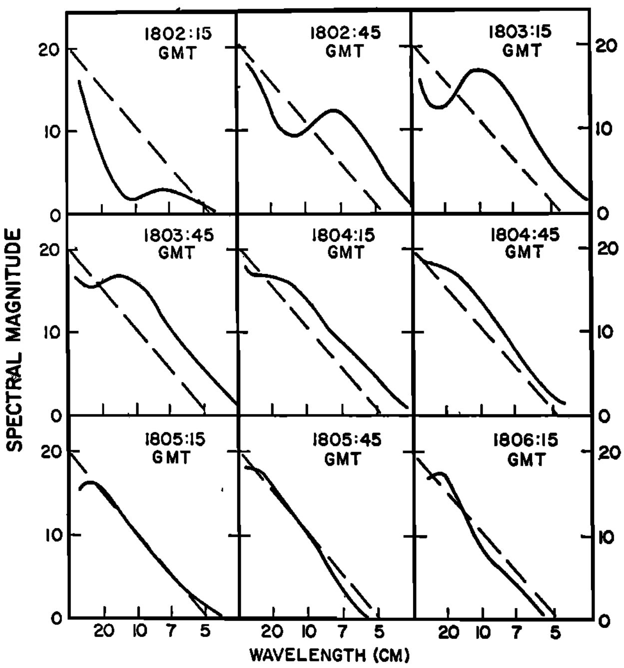

Fig. 4. Temporal variation of K_x spectrum for October 5, 1971.

overshoot. Calculating the equilibrium range constant B' [*Phillips*, 1966] at (for the 18h 06m 15s photograph) 10 and 7 cm gives 2.2×10^{-2} and 1.6×10^{-2}, respectively. These values compare favorably with other experimental values even though the present values may be somewhat contaminated by the proximity of the overshoot tail. The peak overshoot at 10 cm is almost 10 db.

Figure 5 illustrates a part of the directional spectrum for the 18h 03m 15s photograph. The contours are labeled in db greater than 10^{-2} cm² rad². The failure of the contours to close at the 60° azimuth points is probably due to the low signal to noise ratios, 0 db also represents the 0-db signal to noise ratio point. In addition, the $\sec^2 \Psi$ correction factor arising in the wave visibility equations is probably not valid at this azimuth and further amplifies the noise level. The photo was taken looking due west, the 0° direction. The spectral peak is in a direction 15° south of west and agrees with the anemometer. The beam width of the spectrum is approximately 60° at 10 cm.

CONCLUSIONS

The development leading to (33) includes numerous assumptions that influence the applicability of the technique and the accuracy of the spectral estimates obtained. Among these assumptions are small wave slopes, insignificant whitecapping, smooth sky luminance variation in both elevation and azimuth, and an insignificant haze level. These conditions are not severely restrictive. The distribution of wave slopes is such that slopes sufficiently large to introduce significant errors into the analysis occur infrequently and only at a small set of points in the image of the waves. Only at wind speeds in excess of 12 m/s does the fractional whitecap coverage become sufficiently great to preclude useful photos. Even with a sky consisting of broken clouds the subresolution waves allow estimates of the spectrum of long water wavelengths.

Most of the difficulties become critical only in attempting to study capillary waves. In this case there are very few smaller waves to smooth the sky luminance discontinuities, and steep slopes are the rule rather than the exception. Further, the shutter speed required for the camera to stop the motion becomes high. With presently available films and lenses the available light creates exposure problems. At very low sea states the technique should also prove useful for the capillaries.

The experimental results are indicative of the kinds of measurements possible with optical techniques that were not heretofore readily available. In sea states corresponding to winds less than 12 m/s the optically derived spectrum should be useful. Proper experimental design can elicit wave information over a protracted range of wavelengths. The camera system can be modified somewhat to provide very accurate information on waves in wave tanks. With precise ancillary measurements a good deal of the physics of wave propagation, interaction, and generation should be open to investigation. The potential of examining both the nonstationary quality and the inhomogeneity of the spectrum should prove particularly useful in such programs.

APPENDIX 1: SPECTRAL DEFINITIONS AND NOTATION

It is necessary to adapt the definitions of spectra to a form suitable for optical analysis of wave photographs. This can be done by relating the Fourier transform of a function to a realizable estimator of the transform and then by defining the spectrum as a function of the Fourier transform. For the purposes of this paper the Fourier transforms

$$\mathfrak{F}\{H(\mathbf{X})\} = \bar{H}(\mathbf{K}) = \iint_{-\infty}^{\infty} H(\mathbf{X}) \exp(-2\pi i \mathbf{K}\cdot\mathbf{X})\, d\mathbf{X} \qquad \text{(A1)}$$

$$\mathfrak{F}^{-1}\{\bar{H}(\mathbf{K})\} = H(\mathbf{X}) = \iint_{-\infty}^{\infty} \bar{H}(\mathbf{K}) \exp(2\pi i \mathbf{K}\cdot\mathbf{X})\, d\mathbf{K} \qquad \text{(A2)}$$

are used. It should be noted that fractional wave numbers are used rather than the more common radian measure.

One of the major problems encountered in Fourier analysis is that the above definitions extend over an infinite domain, whereas experimentally accessible functions are restricted to a finite domain. To avoid this difficulty, the integrand can be weighted by a function that is zero outside of a finite interval. With the proper class of weight functions the resulting transforms are easily interpretable in terms of an estimator of

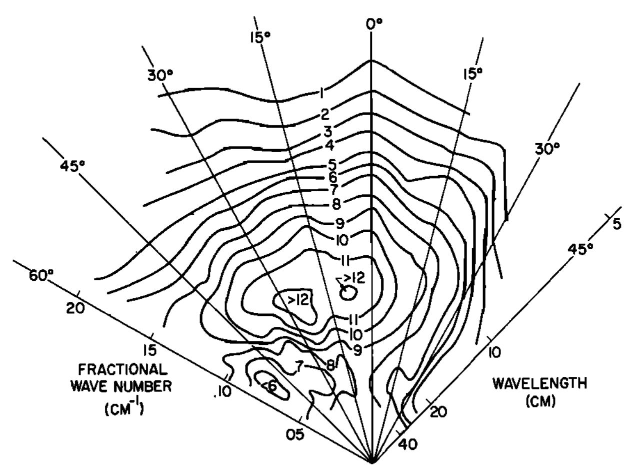

Fig. 5. Directional spectrum for October 5, 1971.

the spectrum. To exemplify this procedure, consider the transform (in one dimension only)

$$\mathfrak{F}\{H(X)G(X)\} = \int_{-\infty}^{\infty} H(X)G(X) \exp(-2\pi i K X)\, dX$$
$$= \int_{-\infty}^{\infty} \bar{H}(K)\bar{G}(K - K_0)\, dK_0 \quad \text{(A3)}$$

where $G(x)$ is a Gaussian function defined by

$$G(X) = \exp(-X^2/2\sigma^2)$$
$$\bar{G}(K) = (2\pi)^{1/2}\exp(-2\pi^2\sigma^2K^2) \quad \text{(A4)}$$

The $\bar{G}(K)$ factor in the integrand of the convolution integral can be approximated by using the concept of equivalent widths [*Bracewell*, 1965]

$$\frac{\int_{-\infty}^{\infty} \bar{G}(K)\, dK}{\bar{G}(0)} = \frac{G(0)}{\int_{-\infty}^{\infty} G(X)\, dX} = \delta K = \frac{1}{\delta X} \quad \text{(A5)}$$

and where

$$G(0) = \int_{-\infty}^{\infty} \bar{G}(K)\, dK \quad \text{(A6)}$$

Equations A5 and A6 apply for a large class of functions and not simply for Gaussian functions. Then

$$\mathfrak{F}\{H(X)G(X)\} \cong \bar{G}(0) \int_{K}^{K+\delta K} \bar{H}(K)\, dK$$
$$= G(0)\left[\frac{1}{\delta K}\int_{K}^{K+\delta K} \bar{H}(K)\, dK\right] \equiv G(0)\langle \bar{H}(K)\rangle \quad \text{(A7)}$$

where the term in angle brackets is defined to be the estimator of the transform $\bar{H}(K)$. The estimator can be expected to be good in the range of K, for which $\bar{G}(K) \ll \bar{H}(K)$.

The spectrum can now be defined in terms of the Fourier transform as follows. The variance of a function $H(\mathbf{X})$ over a two-dimensional region $\delta\mathbf{X}$ is

$$\langle H^2(\mathbf{X})\rangle = \frac{1}{\delta\mathbf{X}} \int_{\delta\mathbf{X}} H^2(\mathbf{X})\, d\mathbf{X} \quad \text{(A8)}$$

The spectrum is defined to be the quantity $\Phi(H; \mathbf{K})$, which yields

$$\langle H^2(\mathbf{X})\rangle = \iint_{-\infty}^{\infty} \Phi(H; \mathbf{K})\, d\mathbf{K} \quad \text{(A9)}$$

Using Parseval's theorem in (A8) yields

$$\langle H^2(\mathbf{X})\rangle = \frac{1}{\delta\mathbf{X}} \iint_{-\infty}^{\infty} \bar{H}^2(\mathbf{K})\, d\mathbf{K} \quad \text{(A10)}$$

which can be cast into the form

$$\langle H^2(\mathbf{X})\rangle = \iint_{-\infty}^{\infty} \left[\iint_{\mathbf{K}}^{\mathbf{K}+\delta\mathbf{K}} \bar{H}^2(\mathbf{K})\, d\mathbf{K}\right] d\mathbf{K} \quad \text{(A11)}$$

with $\delta\mathbf{K}\ \delta\mathbf{X} = 1$, and then

$$\Phi(H; \mathbf{K}) = \iint_{\mathbf{K}}^{\mathbf{K}+\delta\mathbf{K}} \bar{H}^2(\mathbf{K})\, d\mathbf{K} \quad \text{(A12)}$$

The spectrum thus incorporates the effects of the finite boundaries of the region. The wave number interval $\delta\mathbf{K}$ defines the smallest independent wave number interval commensurate with the data and represents a region in wave number space comprising one equivalent chi-squared variable; i.e., a single degree of freedom.

The notation $\Phi(A; B_i)$ is used to denote the spectrum of A as a function of the set of parameters B_i. The vector notation of the differential elements in (A1 and A2) may denote either spatial, temporal, or mixed variables. Dimensionally the spectrum is determined by the dimensions of A^2 divided by the dimensions of the surface specified by the B_i. In particular, $\Phi(\phi; K_x, K_y) = \Phi(\phi; \mathbf{K})$ denotes the spectrum of the normal angle of the surface as a function of the directional wave numbers and has units of L^2; $\Phi(\tan\Phi; K, \Psi)$ denotes the slope spectrum as a function of the wave number magnitude K and the azimuth angle Ψ with units L^2. The $\Phi(H; \omega)$ denotes the wave height spectrum as a function of the radian frequency ω and has units L^2T/rad; $\Phi(H; \mathbf{K})$ denotes the wave height spectrum as a function of directional wave number with dimensions L^4. As is implied from these definitions, there are a number of spectra and surface descriptors applicable to any given surface. Those of primary importance are the wave height, the slope, and the wave normal angle. The relationship between the various derived spectra is given approximately by $\Phi(\phi; K_x, K_y) = \Phi(\tan\phi; \mathbf{K}) = K^2\Phi(H; K, \Psi)$; with the additional condition, valid only in the gravity wave range, $\omega^2 = 2\pi gK$, where g is the acceleration of gravity, one can determine [*Kinsman*, 1965]

$$\Phi(H; \omega) = \frac{2\omega^3}{g^2} \int_0^{2\pi} \Phi(H; K, \Psi)\, d\Psi$$

APPENDIX 2: THREE-DIMENSIONAL GEOMETRY

Figure 6 shows a sketch of the local geometry at a point on the ocean surface. The camera is located in the direction $\hat{C}$, the reflected ray comes from the sky from the direction $\hat{S}$, and the refracted ray comes from the water in the direction $\hat{W}$. The angles η, ϕ, and η' are measured with respect to the axis for the sky, normal angle, and water rays, respectively. They are given by

$$\cos\eta = \hat{K}\cdot\hat{S}$$
$$\cos\phi = \hat{K}\cdot\hat{N} \quad \text{(A13)}$$
$$\cos\eta' = \hat{K}\cdot\hat{W}$$

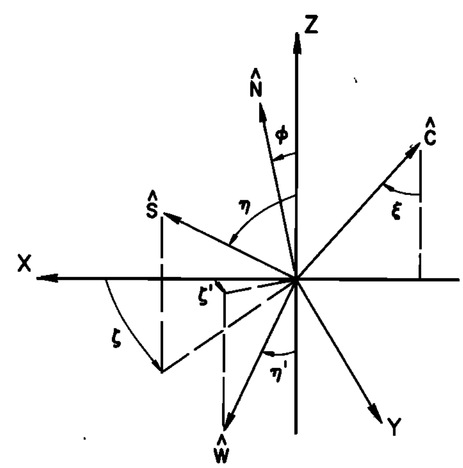

Fig. 6. The three-dimensional local geometry for the reflected and transmitted light rays.

The effective angle of reflection β is given by

$$\cos\beta = \hat{N}\cdot\hat{C} \tag{A14}$$

The angles ζ, Ψ, and ζ' are the angles formed by the horizontal projections of the sky, normal, and water rays, respectively, with the x axis and are given by the equations

$$\begin{aligned} \cos\zeta &= \hat{\imath}\cdot(\sin\eta)^{-1}\,\hat{S} \\ \cos\Psi &= \hat{\imath}\cdot(\sin\phi)^{-1}\,\hat{N} \\ \cos\zeta' &= \hat{\imath}\cdot(\sin\eta')^{-1}\,\hat{W} \end{aligned} \tag{A15}$$

With the set of equations

$$\begin{aligned} \hat{N} &= \hat{\imath}\sin\phi\cos\Psi + \hat{\jmath}\sin\phi\sin\Psi + \hat{k}\cos\phi \\ \hat{C} &= -\hat{\imath}\sin\xi + \hat{k}\cos\xi \\ \hat{S} &= -\hat{C} + 2(\hat{N}\cdot\hat{C})\hat{N} \\ n\hat{W} &= -\hat{C} + \hat{N}(\hat{N}\cdot\hat{C} + \hat{N}\cdot\hat{W}) \\ \hat{N}\cdot\hat{W} &= \cos\beta' \\ \sin\beta' &= (1/n)\sin\beta \end{aligned}$$

there is a unique solution for the unknown angles η, η', ζ, and ζ'.

APPENDIX 3: SPECTRUM SCALING

Consider an exact model of the ocean surface that existed at some time. Measurements made on the model can be scaled to yield the spectral properties of the real ocean. With the scaling factors from the sea to the model

$$H = M_z h \qquad M_x x = X \qquad M_y y = Y \tag{A16}$$

where the capital letters refer to the sea, and the small letters to the model. The application of the basic Fourier transform equations

$$\begin{aligned} \bar{H}(K_x, K_y) &= \iint H(X, Y) \\ &\quad\cdot\exp\,[-2\pi i(K_x X + K_y Y)]\,dX\,dY \\ \bar{h}(k_x, k_y) &= \iint h(x, y) \\ &\quad\cdot\exp\,[-2\pi i(k_x x + k_y y)]\,dx\,dy \end{aligned} \tag{A17}$$

yields

$$\bar{h}(k_x, k_y) = \bar{h}(M_x K_x, M_y K_y) = (M_z M_x M_y)^{-1}\bar{H}(K_x, K_y) \tag{A18}$$

Then since

$$\Phi_{\mathrm{model}}(M_x K_x, M_y K_y) = \iint |\bar{h}|^2\,dk_x\,dk_y \tag{A19}$$

and

$$\Phi_{\mathrm{ocean}}(K_x, K_y) = \iint |\bar{H}|^2\,dK_x\,dK_y \tag{A20}$$

one obtains

$$\Phi_{\mathrm{ocean}}(K_x, K_y) = M_x M_y M_z^2 \Phi_{\mathrm{model}}(M_x K_x, M_y K_y) \tag{A21}$$

or in polar form

$$\begin{aligned} \Phi_{\mathrm{ocean}}(K_x, K_y) = M_x M_y M_z^2 \Phi_{\mathrm{model}}([M_x^2\cos^2\Psi \\ + M_y^2\sin^2\Psi]^{1/2}K, \Psi) \end{aligned} \tag{A22}$$

REFERENCES

Barber, N. F., A diffraction analysis of a photograph of the sea, *Nature, 164*, 458, 1949.

Bracewell, R., *The Fourier Transform and its Application*, p. 148, McGraw-Hill, New York, 1965.

Cox, C., and W. Munk, Measurements of the roughness of the sea surface from photographs of the sun's glitter, *J. Opt. Soc. Amer., 44*(11), 838–850, 1954.

Goodman, J. W., *Introduction to Fourier Optics*, p. 88, McGraw-Hill, New York, 1968.

Kinsman, B., *Wind Waves*, p. 341, Prentice-Hall, Englewood Cliffs, N. J., 1965.

Neuman, G., and W. J. Pierson, Jr., *Principles of Physical Oceanography*, p. 331, Prentice-Hall, Englewood Cliffs, N. J., 1966.

Pierson, W. J., The directional spectrum of a wind generated sea as determined from data obtained by the stereo wave observation project, *N. Y. Univ. Meteorol. Pap., 2*(6), 1960.

Phillips, O. M., *The Dynamics of the Upper Ocean*, p. 120, Cambridge University Press, London, 1966.

Stilwell, D., Jr., Directional energy spectra of the sea from photographs, *J. Geophys. Res., 74*(8), 1974–1986, 1969.

(Received March 30, 1973;
revised January 3, 1974.)